

Submicron Structure in L- α -Dipalmitoylphosphatidylcholine Monolayers and Bilayers Probed with Confocal, Atomic Force, and Near-Field Microscopy

Christopher W. Hollars and Robert C. Dunn

Department of Chemistry, University of Kansas, Lawrence, Kansas 66045 USA

ABSTRACT Langmuir-Blodgett (LB) monolayers and bilayers of L- α -dipalmitoylphosphatidylcholine (DPPC), fluorescently doped with 1,1'-dioctadecyl-3,3,3',3'-tetramethylindocarbocyanine perchlorate (diI-C₁₈), are studied by confocal microscopy, atomic force microscopy (AFM), and near-field scanning optical microscopy (NSOM). Beyond the resolution limit of confocal microscopy, both AFM and NSOM measurements of mica-supported lipid monolayers reveal small domains on the submicron scale. In the NSOM studies, simultaneous high-resolution fluorescence and topography measurements of these structures confirm that they arise from coexisting liquid condensed (LC) and liquid expanded (LE) lipid phases, and not defects in the monolayer. AFM studies of bilayers formed by a combination of LB dipping and Langmuir-Schaefer monolayer transfer exhibit complex surface topographies that reflect a convolution of the phase structure present in each of the individual monolayers. NSOM fluorescence measurements, however, are able to resolve the underlying lipid domains from each side of the bilayer and show that they are qualitatively similar to those observed in the monolayers. The observation of the small lipid domains in these bilayers is beyond the spatial resolving power of confocal microscopy and is complicated in the topography measurements taken with AFM, illustrating the utility of NSOM for these types of studies. The data suggest that the small LC and LE lipid domains are formed after lipid transfer to the substrate through a dewetting mechanism. The possible extension of these measurements to probing for lipid phase domains in natural biomembranes is discussed.

INTRODUCTION

The continuing evolution in fields such as microelectronics and optics has led to a renewed interest in the study of thin organic films (Roberts, 1990; Sackmann, 1996; Swalen et al., 1987). Organic films, formed on surfaces through the Langmuir-Blodgett (LB) technique, often exhibit interesting surface-modifying properties that show promise in areas such as nonlinear optics, photoresists and electrode modifying agents, and as passivating barriers for reducing surface corrosion (Roberts, 1990; Sackmann, 1996; Tollner et al., 1997). Despite their potential in these areas, however, their use in practical devices has been slowed by their inherent fragility and susceptibility to defects and impurities in the film structure (Swalen et al., 1987). These difficulties, along with a fundamental interest in the structure of these films, have driven research aimed at understanding their microscopic properties.

Much of this research is focused on the microscopic structure of phospholipid films. Phospholipids are ubiquitous in biological membranes, and their LB films often exhibit interesting two-dimensional phase partitioning that may play important functional roles in cellular membranes (Gennis, 1989; Lehtonen and Kinnunen, 1995; Tocanne et al., 1994; Vaz and Almeida, 1993). As such, the phase transitions and structures in Langmuir films formed from

lipids at the air-water interface or Langmuir-Blodgett films of supported lipids have been studied extensively.

As the surface area of a lipid monolayer confined at the air-water interface is reduced, two-dimensional phase transitions occur that correspond to structural changes taking place in the lipid monolayer (Gaines, 1966; Gennis, 1989). These changes can be probed by a variety of techniques. Perhaps the most general and widely utilized technique for monitoring the phases present in LB films is fluorescence microscopy (Knobler, 1990; Lösche et al., 1983, 1984; McConnell et al., 1984; Möhwald, 1990). Fluorescent probe molecules, which have a propensity to partition into a distinct lipid phase, are doped into the lipid film in small molar ratios, thus providing a convenient marker for the coexisting phases present in the film. These studies have provided a wealth of information about the micron scale structures present in lipid films formed under a variety of conditions. However, because of the resolution constraints inherent in conventional optical microscopy, these methods provide little information about the submicron structure. To obtain higher resolution information, many of the newer scanning probe techniques have been successfully implemented at the nanometric dimension. These techniques include methods such as atomic force microscopy (AFM) (Bourdieu et al., 1993; Chi et al., 1993; Mikrut et al., 1993; Yang et al., 1994a,b, 1995), the related frictional force microscopy (Bhushan et al., 1995; Knapp et al., 1995; Overney et al., 1992), and, more recently, near-field scanning optical microscopy (NSOM) (Hollars and Dunn, 1997; Hwang et al., 1995; Moers et al., 1994; Tamm et al., 1996). With these techniques, a detailed view of the submicron properties of lipid films is beginning to emerge.

Received for publication 14 January 1998 and in final form 9 April 1998.

Address reprint requests to Dr. Robert C. Dunn, Department of Chemistry, University of Kansas, Malott Hall, Lawrence, KS 66045-0046. Tel.: 913-864-4313; Fax: 913-864-5396; E-mail: rdunn@caco3.chem.ukans.edu.

© 1998 by the Biophysical Society

0006-3495/98/07/342/12 \$2.00

Typically, contrast in the AFM studies arises from the changes in height associated with the coexisting lipid phases. For example, monolayers of DPPC deposited on substrates in the liquid expanded (LE)–liquid condensed (LC) coexistence region exhibit height changes of ~ 5 – 25 Å in going from the tilted LE phase to the more upright LC phase (Hollars and Dunn, 1997; Masai et al., 1996; Yang et al., 1994a,b, 1995). Similar height changes occur in many phase-separated LB films, leading to a useful and general approach to mapping the phase structures present. However, because the AFM technique provides mainly topographical information, interpretation of the images can be complicated by defects in the film structure. Moreover, as the complexity of the film is increased, as in the case of a lipid bilayer, assignments of phase based solely on topographical information can become problematic (Dufrene et al., 1997; Fang and Yang, 1997). Recently, several reports have appeared which suggest that the NSOM technique may provide a complementary view of the lipid phase structure and offer new insights into the submicron structures (Hollars and Dunn, 1997; Hwang et al., 1995; Moers et al., 1994; Tamm et al., 1996). NSOM provides both high-resolution fluorescence and topographic information, which removes many of the ambiguities that can cloud the interpretation of results based on only one of these contrast mechanisms.

NSOM circumvents the spatial resolution constraints encountered in conventional optical microscopy by scanning a small light source close to a sample surface (Betzig et al., 1991; Paesler and Moyer, 1996; Pohl, 1991). NSOM has been applied to the study of single molecules (Ambrose et al., 1994; Betzig and Chichester, 1993; Trautman et al., 1994; Xie and Dunn, 1994), aggregates and solid-state systems (Buratto et al., 1994; Grober et al., 1994; Harris et al., 1996; Higgins and Barbara, 1995), biological samples (Betzig et al., 1993; Dunn et al., 1994, 1995; Enderle et al., 1997; Ha et al., 1996; Talley et al., 1996; van Hulst and Moers, 1996), and recently, LB films (Hollars and Dunn, 1997; Hwang et al., 1995; Moers et al., 1994; Tamm et al., 1996), all with submicron spatial resolution. As an example, NSOM has recently been useful in identifying new structures present in phase-separated DPPC monolayers (Hollars and Dunn, 1997; Hwang et al., 1995). We have utilized NSOM to study DPPC monolayers formed on a glass surface and showed that the phases present in the monolayer can be identified by comparing both the fluorescence and topography images collected with NSOM (Hollars and Dunn, 1997). However, in that study, the inherent roughness of the glass surface supporting the monolayer, combined with the small 5 – 10 Å height difference between the LE and LC lipid phases, complicated a direct comparison between the fluorescence and topographic images for some of the smaller lipid domains. Nevertheless, these results demonstrated the advantage of probing the lipid phase structure with NSOM by using both the fluorescence signature, used extensively in fluorescence microscopy studies, and the topographic changes, exploited in AFM studies.

Here we extend our initial report by studying the coexisting LE/LC phase structure present in DPPC films deposited on freshly cleaved mica surfaces. The atomically flat mica surface allows the coexisting lipid phases in a DPPC monolayer to be unambiguously assigned by comparing both the fluorescence and topography images collected with NSOM. Results from confocal, AFM, and NSOM measurements on both DPPC monolayers and bilayers are compared, illustrating the unique capabilities of NSOM for these types of studies. Beyond the spatial resolution of confocal microscopy, both AFM and NSOM reveal small lipid islands in the “LE” areas of DPPC monolayers transferred in the LC/LE coexistence region. These small structures have been observed previously in AFM studies and assigned to either distinct coexisting lipid phases or defects in the monolayer (Chi et al., 1993; Fang and Knobler, 1995; Santesson et al., 1995; Sikes and Schwartz, 1997; Yang et al., 1994a,b, 1995). Because of the atomically flat mica surface, however, a direct comparison can be made between the high-resolution force and fluorescence images collected with NSOM, which confirms that the domains arise from coexisting lipid phases.

For more complicated films, such as lipid bilayers, the NSOM fluorescence images provide a unique view of the submicron structures present on either side of the lipid bilayer. Small domains, similar to those seen in the monolayers, are observed in the NSOM fluorescence images from both sides of the lipid bilayer. These structures are not visible in the confocal measurements, because of limitations in spatial resolution, and are obscured in the AFM measurements because of the increased complexity of the membrane topography. Comparing the results from films transferred onto a variety of substrates and utilizing different transfer techniques suggest that the formation of the small lipid domains arises from a dewetting mechanism following film transfer. The results shown here for both lipid monolayers and bilayers illustrate the unique capabilities of NSOM in probing small lipid structures. These measurements are discussed in light of future experiments aimed at probing similar structures in natural biomembranes.

MATERIALS AND METHODS

L- α -Dipalmitoylphosphatidylcholine (DPPC) (Sigma) and 1,1'-dioctadecyl-3,3,3',3'-tetramethylindocarbocyanine perchlorate (diI_{18}) (Molecular Probes) were used without further purification. DPPC was dissolved in spectral grade chloroform (1 mg/ml), into which a small volume of a concentrated solution of diI_{18} in methanol was added to a final concentration of 0.25 mol%. The lipid mixture was dispersed onto a 10 mM aqueous MgCl_2 subphase and compressed to a surface pressure of 9 mN/m with a computer controlled Langmuir-Blodgett trough (model 611; Nima Technology) equipped with a Wilhelmy pressure sensor. The compression rate was $100 \text{ cm}^2/\text{min}$, and the films were transferred onto freshly cleaved mica surfaces at a dipping velocity of 25 mm/min. The mica substrate was immersed in the subphase and pulled through the air-water interface to transfer the lipid monolayer in a headgroup down structure. For Y-type bilayer formation, the second lipid monolayer was transferred under the same conditions with the Langmuir-Schaefer technique.

The lipid films were imaged with a custom-built microscope capable of confocal microscopy, atomic force microscopy, and near-field scanning

optical microscopy (Talley et al., 1996). Briefly, the microscope is similar in design to the commercially available Bioscope atomic force microscope from Digital Instruments. The Bioscope is mounted on an inverted fluorescence microscope (Zeiss Axiovert 135TV) equipped with either a Zeiss fluar 40 \times (1.3 NA) or 100 \times (1.3 NA) oil immersion objective lens. For near-field measurements, cantilevered near-field fiber optic probes are fabricated as previously described (Talley et al., 1996) and mounted in a Dimension AFM head (Digital Instruments). For contact-mode AFM measurements, silicon nitride tips with a force constant of ~ 0.06 N/m were used in the imaging. For confocal and near-field measurements, the sample is scanned using a separate x - y closed-loop piezo scanner (Physik Instrumente). Excitation light in these experiments is provided by an argon ion laser (Liconix 5000) operating at the 514-nm line. Fluorescence from the sample is collected from below the sample with the high-NA objective lens, filtered to remove residual excitation light, and imaged on an avalanche photodiode detector (EG&G, SPCM-200). For all experiments, piezo scanning and data acquisition were controlled with a Digital Instruments Nanoscope IIIa control station and software.

RESULTS

The pressure isotherm for DPPC/0.25 mol% diIC₁₈ is shown in Fig. 1, along with the point on the isotherm (9 mN/m) at which the films were transferred onto a freshly cleaved mica surface. This part of the isotherm corresponds to a phase coexistence region where the DPPC monolayer contains both liquid-condensed (LC) and liquid-expanded (LE) phases (Cadenhead et al., 1980). This can be seen in Fig. 2 *A*, which shows a typical 35 $\mu\text{m} \times 35 \mu\text{m}$ confocal fluorescence image of a DPPC/0.25 mol% diIC₁₈ monolayer transferred onto a mica surface. Previous studies have shown that diIC₁₈ preferentially partitions into the LE phase, providing a convenient marker for the LC/LE phase

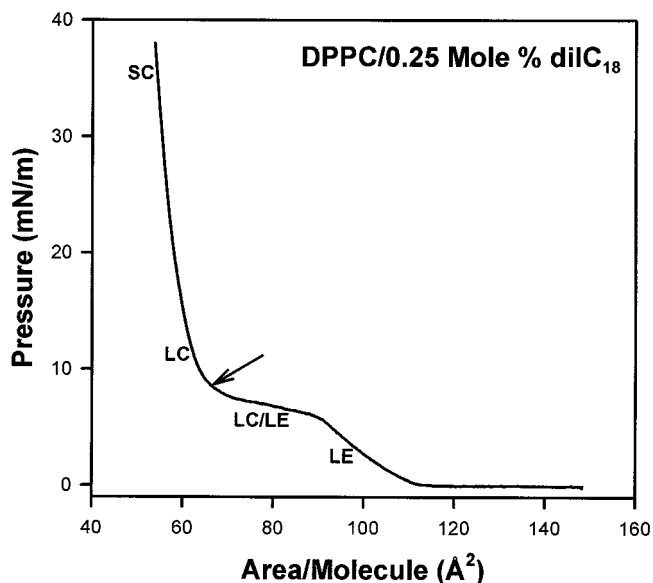


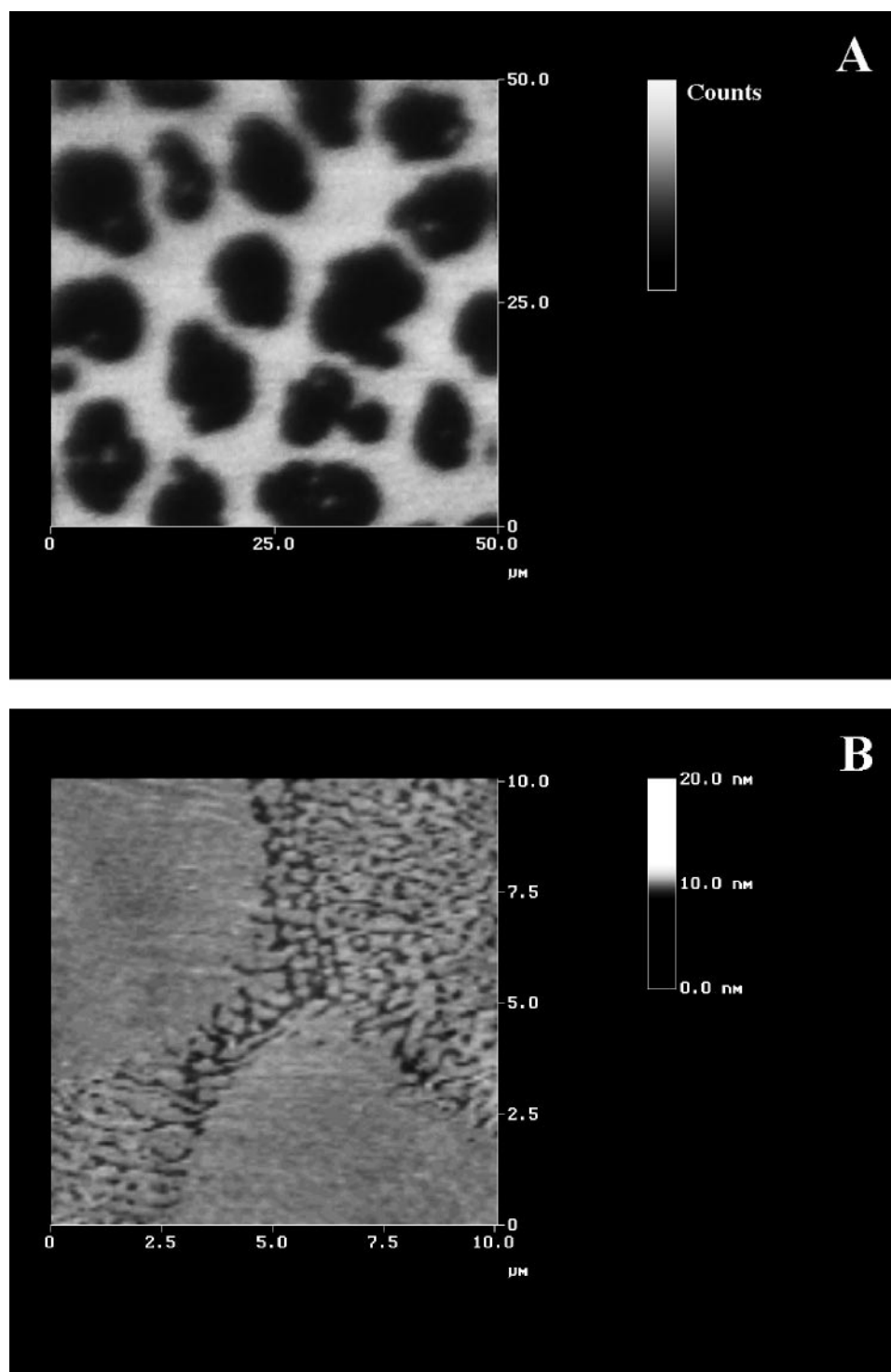
FIGURE 1 Room temperature pressure/area isotherm of DPPC/0.25 mol% diIC₁₈ on a 10 mM MgCl₂ subphase. The different regions along the curve are identified as SC (solid condensed), LC (liquid condensed), LC/LE (liquid condensed/liquid expanded), and LE (liquid expanded), which reflects the predominant lipid phase present. The arrow marks the pressure (9 mN/m) at which the monolayers were transferred onto a freshly cleaved mica substrate.

distribution present in the monolayer (Derzko and Jacobson, 1980; Hollars and Dunn, 1997; Lösche et al., 1983). In Fig. 2 *A*, the nonfluorescent circular domains, indicative of the LC lipid phase, are surrounded by the fluorescently doped, apparently homogeneous LE regions. Many studies of this type have been reported, and the phase distributions have been characterized as a function of physical parameters, such as temperature and surface pressure, as well as chemical constituents added to the lipid, such as cholesterol (Lösche et al., 1983; McConnell, 1991; McConnell et al., 1984; Möhwald, 1990; Roberts, 1990). In general, the equilibrium size and shape of the domains are governed by a balance between the line tension energy at the phase boundaries and longer range dipole-dipole interactions between the lipids.

With the higher magnification possible with AFM, new features in the lipid monolayer can be revealed. Fig. 2 *B* shows a 10 $\mu\text{m} \times 10 \mu\text{m}$ AFM image of the same monolayer imaged with confocal microscopy in Fig. 2 *A*. The large circular LC domains seen in the confocal image are also evident in the AFM image and appear to be ~ 5 – 8 Å higher than the surrounding LE regions. This height difference is consistent with previous scanning probe (Hollars and Dunn, 1997; Masai et al., 1996; Yang et al., 1994a,b, 1995) and ellipsometry measurements (Lösche et al., 1984), although there is less agreement among the AFM studies, because of the differing imaging conditions. As shown in Fig. 2 *B*, the “LE” region between the circular LC domains, which appears homogeneous in the confocal fluorescence image, actually contains a distribution of smaller domains. These smaller domains have been observed in previous AFM studies on other LB films and interpreted in several ways. Some studies suggest that this interdomain region consists of defects separating small LC lipid regions (Fang and Knobler, 1995; Santesson et al., 1995; Sikes and Schwartz, 1997), whereas others suggest that it arises from the coexistence of LE and LC lipid (Chi et al., 1993; Yang et al., 1994a,b, 1995).

With the simultaneous near-field fluorescence and topography measurements, however, these regions of the DPPC films are confirmed to arise from distinct coexisting lipid phases. Fig. 3, *A* and *B*, shows the simultaneous near-field fluorescence and topography images, respectively, of a 13 $\mu\text{m} \times 13 \mu\text{m}$ region of the same DPPC monolayer. As in the confocal image, the near-field fluorescence image contains large circular LC regions that exclude the fluorescent dye and appear dark. Between these large domains, however, the increased spatial resolution in the NSOM fluorescence measurements reveals structure in the fluorescence that was not evident in the confocal image. As in the AFM image (Fig. 2 *B*), the near-field topography image shown in Fig. 3 *B* clearly reveals the small height differences (5–8 Å) associated with the coexisting lipid phases. These small changes in topography are easily observed with the high signal-to-noise available in the force image when the NSOM is operated in a tapping-mode arrangement with cantilevered fiber optic probes (Muramatsu et al., 1995;

FIGURE 2 (A) Confocal fluorescence image ($35\ \mu\text{m} \times 35\ \mu\text{m}$) of a mica-supported DPPC/0.25 mol% diI $_{18}$ monolayer. The diI $_{18}$ fluorescent probe preferentially partitions into the LE phase, providing a marker for these regions. The dark, circular regions are LC domains that exclude the fluorescent probe. The LE regions (*bright*) appear homogeneous in this image. (B) AFM image ($10\ \mu\text{m} \times 10\ \mu\text{m}$) of the monolayer shown in A. AFM is sensitive to the small height changes ($5\text{--}8\ \text{\AA}$) associated with going from the tilted LE phase to the upright LC phase. The higher resolution AFM image shows that the apparently homogeneous “LE” regions observed in A actually consist of an intermixing of smaller lipid domains.

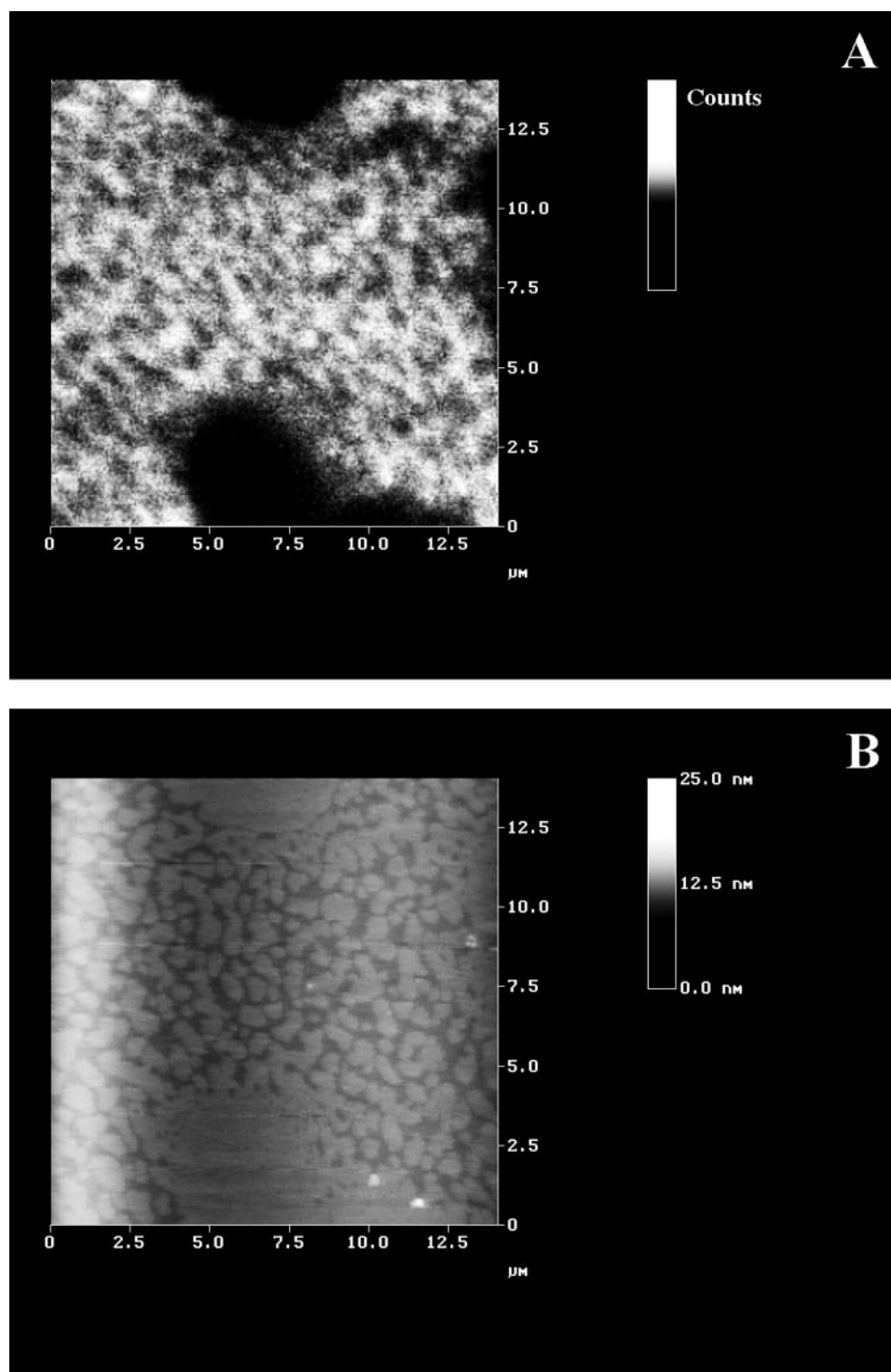


Talley et al., 1996). The two large LC domains of increased height seen in Fig. 3 B correlate directly with the large nonfluorescent regions observed in the simultaneously collected NSOM fluorescence image (Fig. 3 A). Furthermore, the smaller LC domains seen in the “LE” region of Fig. 3 B also exhibit the distinctive height changes expected for coexisting LC and LE phases. The lower topography LE domains (Fig. 3 B) correlate directly with the bright fluorescent features observed in Fig. 3 A, consistent with the

known propensity of diI $_{18}$ to partition into the LE phase. Comparisons between the fluorescence and height data shown in Fig. 3 confirm that the small domains represent a mixture of LC and LE lipid domains and are not due simply to defects in the lipid monolayer.

The collection of both fluorescence and height information with NSOM becomes increasingly important in assigning the lipid phase as the complexity of the sample increases, as in the case of multilayer films. For example,

FIGURE 3 (A) $13\ \mu\text{m} \times 13\ \mu\text{m}$ Near-field fluorescence and (B) topography images of the monolayer shown in Fig. 2. The high resolution in the fluorescence image reveals structure in the LE region, similar to that observed in the AFM image shown in Fig. 2 B. The small 5–8-Å height differences associated with the coexisting lipid phases are observed in the near-field force image shown in B. Regions of high fluorescence in A map the LE domains and directly correlate with the lower height regions in B. This direct comparison between the two images allows for the unambiguous assignment of the small domains to coexisting LE and LC lipid domains.

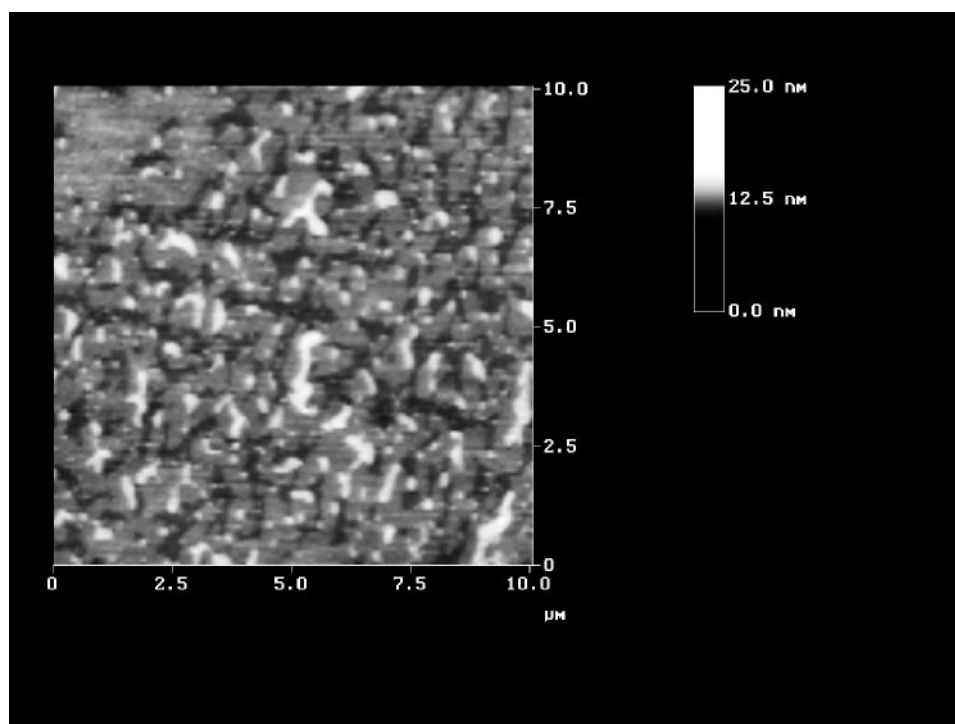


even in the simplest case of a model lipid bilayer, the increased complexity in the surface topography can make lipid phase assignments with AFM problematic. Fig. 4 shows a $10\ \mu\text{m} \times 10\ \mu\text{m}$ AFM image of a DPPC lipid bilayer formed on a mica surface. The first lipid monolayer, consisting of DPPC/0.25 mol% diIC₁₈, was transferred to the mica surface with the headgroups down using the LB dipping technique. The second lipid monolayer, consisting

of pure DPPC, was deposited on top of the first, to form a Y-type bilayer by the Langmuir-Schaefer technique.

The AFM image of the bilayer exhibits discrete height changes in the film topography that occur in multiples of $\sim 8\ \text{\AA}$, approximately equal to the LE/LC height difference seen earlier in the monolayer films. Three quantized height levels are observed, consistent with stackings of LE on LE, LE on LC (or equally LC on LE), and LC on LC in the

FIGURE 4 AFM image ($10\ \mu\text{m} \times 10\ \mu\text{m}$) of a Y-type lipid bilayer formed with the Langmuir-Blodgett technique to transfer the first monolayer (doped with diIC_{18}), followed by the Langmuir-Schaefer technique to transfer the second pure DPPC layer. The film contains three quantized height levels, each $\sim 8\ \text{\AA}$ high. These levels are consistent with stackings of LE on LE, LC on LE (or LE on LC), and LC on LC in the bilayer. Although confocal images of the film show it still contains a macroscopic structure similar to that seen in Fig. 2 *A*, neither the large circular solid domains or smaller coexistence regions are discernible in the complex surface topography.



bilayer. This convolution of topography information from each side of the bilayer obscures the phase structure present in the individual monolayers. It is therefore not immediately apparent from the AFM image shown in Fig. 4 whether the characteristic circular LC domains and mixing of the smaller LE and LC domains remain intact in the bilayer film.

Confocal fluorescence images (not shown), however, reveal that on the micron scale, the phase distributions seen previously for the monolayer films are also present in the bilayer. Each side of the bilayer was doped independently with the fluorescent dye and imaged with confocal microscopy. The results show fluorescence patterns qualitatively similar to that shown in Fig. 2. Therefore, although the topography of the bilayer has been altered to the point where it is not possible to assign the individual domains with any confidence using AFM, confocal fluorescence measurements can still delineate the macroscopic phase structure present in each side of the bilayer. However, the resolution limit in confocal microscopy still prevents the detection of the smaller domains.

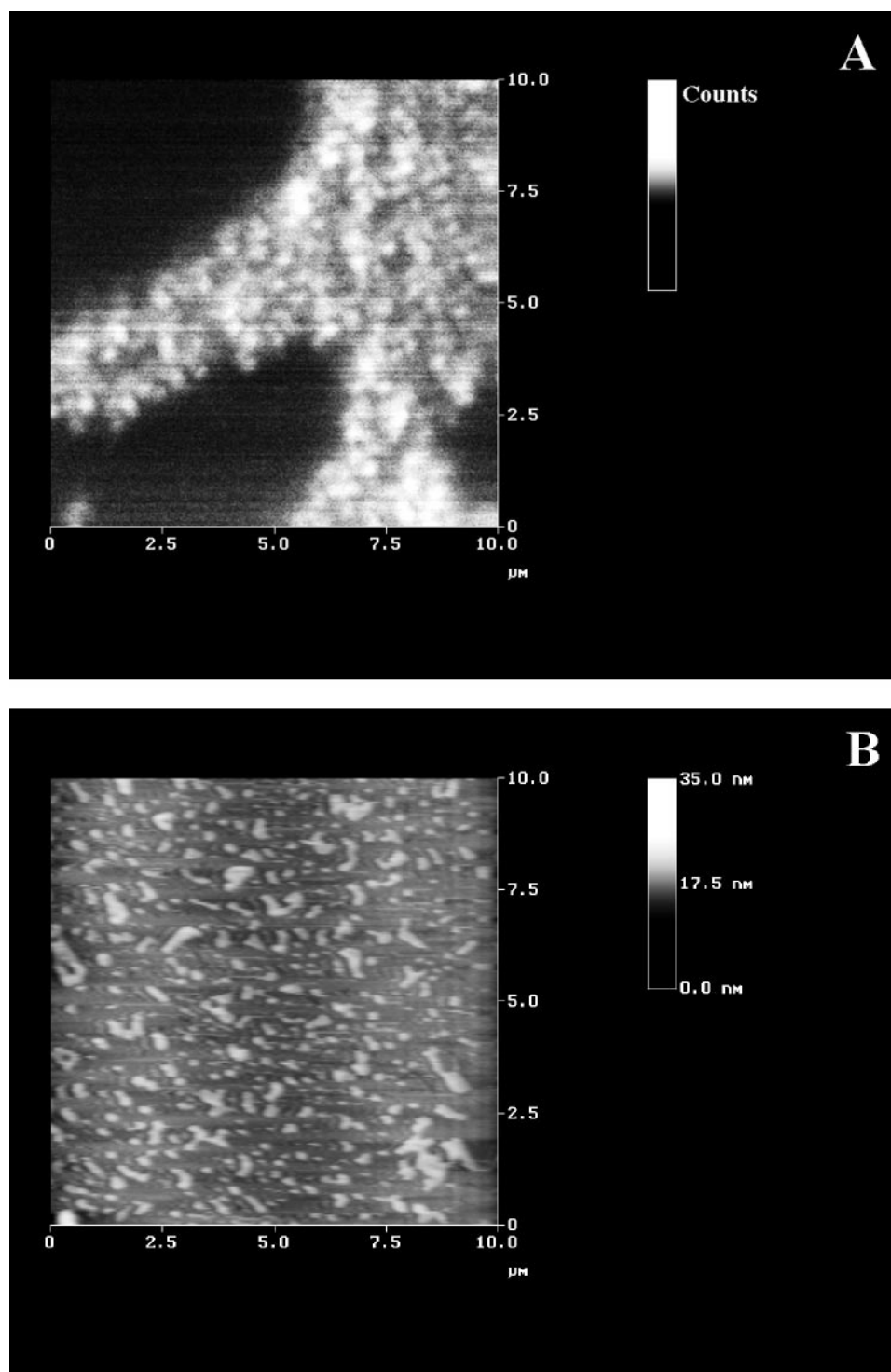
To ascertain whether the small lipid domains observed in the monolayers are also present in the bilayer film, high-resolution NSOM measurements were performed. Fig. 5, *A* and *B*, shows the simultaneous NSOM fluorescence and topography images, respectively, of the same bilayer imaged in the AFM (Fig. 4) and confocal measurements (not shown). The bottom DPPC monolayer is doped with 0.25 mol% diIC_{18} , and the top DPPC monolayer contains no fluorescent dye. As in the AFM image shown in Fig. 4, the near-field topography image shown in Fig. 5 *B* exhibits quantized height changes that reveal no discernible phase

distributions that may exist in the individual monolayers. The simultaneously collected NSOM fluorescence image shown in Fig. 5 *A*, however, clearly shows the distinctive fluorescent patterns seen earlier for the monolayer film. The structure seen in the fluorescence image from the bottom monolayer is qualitatively indistinguishable from that observed for lipid monolayers alone (Figs. 2 and 3). Both the large, circular LC domains and the intermixing of smaller LC and LE domains are observed in Fig. 5 *A*. Similar NSOM fluorescence and topography images, collected on bilayers formed by transferring a pure DPPC monolayer first, followed by a DPPC/0.25 mol% diIC_{18} monolayer on top, are shown in Fig. 6. For this bilayer, the fluorescent probe is in the uppermost monolayer of the film, and the NSOM fluorescence image therefore reflects the phase distributions present in this monolayer. As before, the NSOM fluorescence image detects phase distributions similar to those observed for monolayer films, whereas the force image shows changes in the surface topography that are not correlated with this structure. These results illustrate the capability of NSOM to probe the small phase domains present on either side of the lipid bilayer, which are not evident in either the confocal or AFM measurements.

DISCUSSION

Previous work and the results presented here illustrate the ability of NSOM to probe the small phase structures present in LB films (Hollars and Dunn, 1997; Hwang et al., 1995; Moers et al., 1994; Tamm et al., 1996). The combined high-resolution fluorescence and topographic information

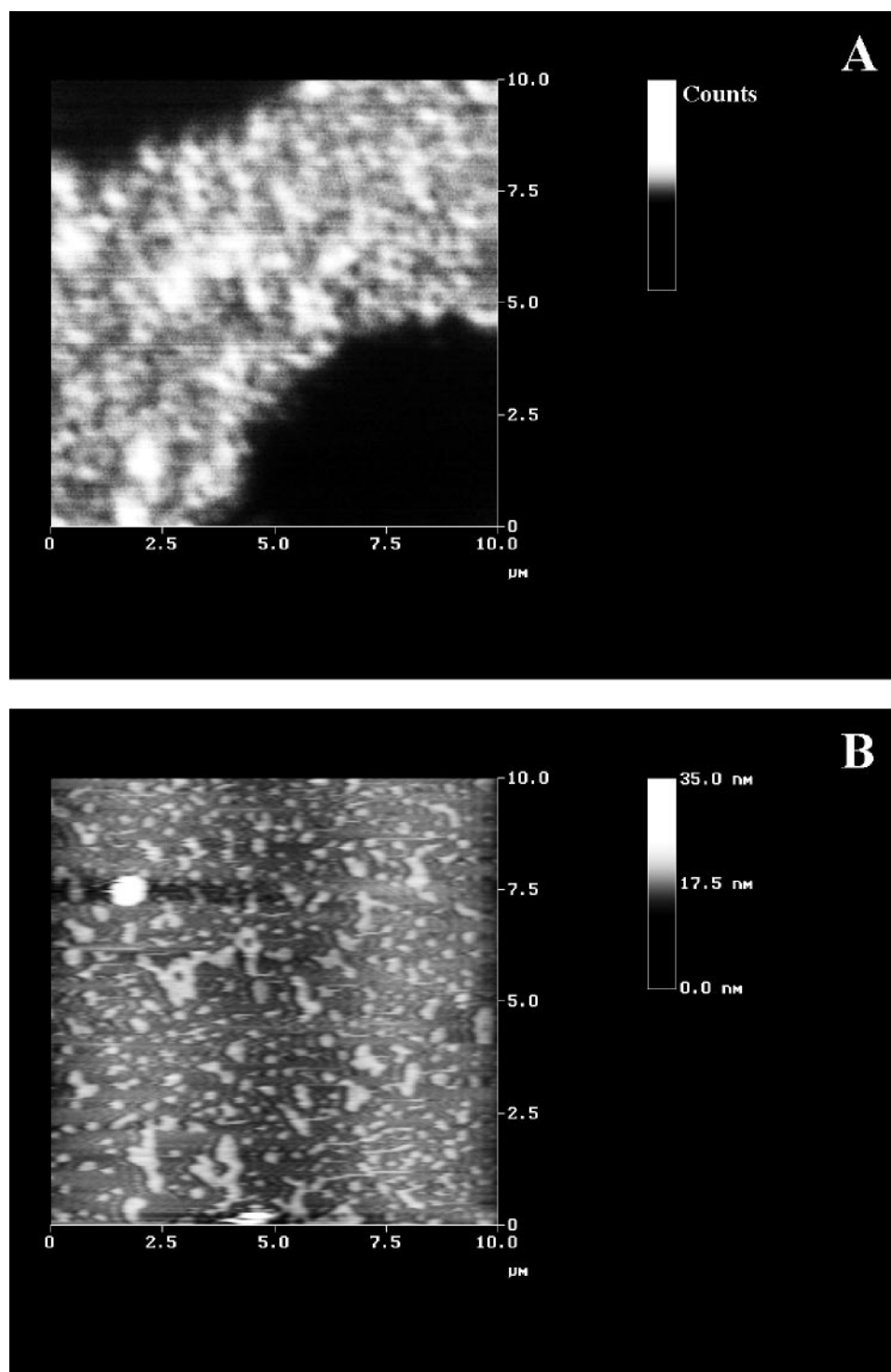
FIGURE 5 (A) $10\ \mu\text{m} \times 10\ \mu\text{m}$ near-field fluorescence and (B) topography images of the same bilayer imaged with AFM in Fig. 4. The near-field topography image (B) exhibits height changes in the film similar to those seen by AFM (Fig. 4). The near-field fluorescence image shown in A, however, reveals the lipid phase structure present in the bottom layer of the bilayer. This structure is qualitatively similar to that seen in the monolayer film (Fig. 3).



provides a self-consistent view of the phase structure present in lipid monolayers (Hollars and Dunn, 1997). For example, in the case of the DPPC monolayer shown in Fig. 3, comparing the lipid topography with the structure seen in the NSOM fluorescence image allows us to unambiguously assign the small features observed in the “LE” region to coexisting LE and LC domains and not simply to defects in the film. As mentioned earlier, previous AFM studies using various contrast mechanisms such as height, friction, and

elasticity have also seen these smaller domains intermingled with the larger LC domains under similar monolayer transfer conditions (Masai et al., 1996; Yang et al., 1994a,b, 1995). We find that these small domains are common features in our samples, regardless of the nature of the substrate. For instance, these domains are observed in lipids transferred onto mica (Figs. 2 and 3), glass (data not shown), and lipid surfaces (Fig. 6), which suggests that their formation is not strongly coupled to the properties of the

FIGURE 6 (A) $10\ \mu\text{m} \times 10\ \mu\text{m}$ near-field fluorescence and (B) topography images of a bilayer formed with the upper layer fluorescently labeled with 0.25 mol% diIC₁₈. As in Fig. 5, the near-field fluorescence image (A) reflects the structure present in the top lipid layer, which is similar to that observed for the DPPC monolayer. The near-field topography image (B) exhibits height changes that are not correlated with the structure observed in the near-field fluorescence image.



underlying substrate for this subphase. The origin of these small domains, however, remains unclear. Are they present at the air-water interface, or simply introduced into the monolayer upon transfer onto the solid support?

In a series of papers, Riegler and co-workers showed that under certain conditions, the phase structure of lipid monolayers can be modified by the dipping procedure that transfers the lipid onto the solid support (Riegler and Spratte, 1992; Riegler and LeGrange, 1988; Spratte and Riegler,

1994). Using a specially designed fluorescence microscope capable of probing various regions of the film during the transfer process, they were able to uncover changes in the phase structure occurring at the substrate/subphase interface. Monolayers composed of dimyristoylphosphatidylethanolamine (DMPE) doped with 1.1% NBD-dihexadecylamine exhibited a local liquid-to-solid phase transition at the meniscus formed between the solid-subphase interface (Riegler and LeGrange, 1988). This phase transition, it was

proposed, arose from local pH variations in this region induced by the limited mixing between ions in the meniscus and those in the bulk solution. Recently similar experiments have found perturbations in the film structure attributable to substrate-mediated condensation. The differing environments of the floating and deposited monolayer at the substrate/subphase interface can lead to local morphology changes in the film (Riegler and Spratte, 1992; Spratte and Riegler, 1994). These mechanisms could possibly result in the formation of the small LC/LE domains observed in Figs. 2 B through 6.

Comparison of the NSOM results for bilayers, shown in Figs. 5 and 6, however, suggests that these mechanisms are not responsible for the small domain formation seen here. In Fig. 5, the NSOM fluorescence image reflects the structure in the bottom lipid layer, transferred by the Langmuir-Blodgett dipping technique. This structure is qualitatively indistinguishable from that seen in Fig. 6, where the NSOM fluorescence image reflects the structure in the upper monolayer, transferred by the Langmuir-Schaefer technique. In Langmuir-Schaefer film transfer, the entire substrate surface is exposed to the air-water interface, and the film is transferred in one step. Local pH variations or an evolution in the film structure due to interactions between bound and free monolayer is not expected in this configuration, because the entire interface is exposed to the monolayer at the same time. It does not appear, therefore, that the small domains observed here are directly related to the film transfer process itself, but result from an evolution in the film structure immediately following transfer onto the substrate.

Studies have shown that LB monolayers can condense upon transfer to a solid support to form solid phase islands (Mikrut et al., 1993; Sikes and Schwartz, 1997; Sikes et al., 1996). This may represent an aggregation process, in which a thinning of the water layer between the monolayer and the substrate leads to island growth of a condensed phase (Fang and Knobler, 1995; Reiter, 1992; Srinivasan et al., 1988). In arid conditions, LB monolayers of L- α -dimyristoylphosphatidic acid on a glass substrate can collapse into multilayer films (Mikrut et al., 1993). In humid conditions, on the other hand, the small lipid domains of DPPC become very mobile on the mica surface and aggregate to form larger domains of like phase (Chen et al., 1989; Shiku and Dunn, 1998). Both results illustrate the mobility of lipid monolayers after transfer onto a solid support. Based on these observations, it is unlikely that the small domains observed here are also present at the air-water interface, but instead are induced in the film by the thinning of the water layer between the lipids and the mica surface.

To unambiguously answer this question, however, it is necessary to probe the film structure at the air-water interface with sufficiently high spatial resolution to resolve the small domains, which, to our knowledge, has not been done. As shown earlier, confocal measurements lack the spatial resolution to resolve the smaller LE/LC lipid domains, which is compounded at the air-water interface by the loss of oil immersion objectives. AFM measurements at the air-

water interface could possibly answer this question, but these measurements remain technically challenging and are unlikely to have the necessary sensitivity and resolution to answer this question soon. NSOM measurements, however, may be able to provide clues to the submicron lipid structure present at the air-water interface by scanning the NSOM tip across the air/water interface at constant height. These experiments are currently under way in our laboratory.

Regardless of the origin of the small domains, the results shown in Figs. 5 and 6 demonstrate that each side of the lipid bilayer can be selectively probed at the submicron level with NSOM, simply by controlling which side is doped with the fluorescent probe. In each case, the NSOM fluorescence image is able to reveal the underlying phase structure of the lipid film, which is not directly correlated with the surface topography observed in the force image. These results are particularly interesting in light of recent studies which suggest that similar small lipid domains may be present in biological membranes (Dupou et al., 1988; Metcalf et al., 1986; Tocanne et al., 1994; Wolf et al., 1988).

There is currently a great deal of interest in understanding the role of lipids in influencing the activity of membrane-bound proteins. Modulations of membrane thickness (Baldwin and Hubbell, 1985; Caffrey and Feigenson, 1981; Criado et al., 1984; Johannsson et al., 1981; Peschke et al., 1987; Peterson and McConnaughey, 1981; Salamon et al., 1994), stiffness (Lundbaek et al., 1996; Peschke et al., 1987), and curvature (Baeza et al., 1994; Chernomordik and Zimmerberg, 1995; Epand and Epand, 1994; Gibson and Brown, 1993; Hui and Sen, 1989; Jensen and Schutzbach, 1984; Kelusky and Smith, 1983; McCallum and Epand, 1995; Navarro et al., 1984; Rilfors et al., 1994; Sackmann, 1994) have all been shown to affect the activity of certain integral proteins. For coexisting lipid phases, if present, these structures may provide a means of sequestering enzymes in unique physical environments (Johnson and Edidin, 1978) or provide topographical organizers for cell membrane receptors. They may also create boundary discontinuities in the membrane to increase passive transport, enhance pore development, or promote the fusing of lipid vesicles to the membrane. Fluorescence recovery after photobleaching (FRAP) studies on membranes from soybean protoplast (Metcalf et al., 1986), cultured rose (Walko and Nothnagel, 1989), and maize (Dugas et al., 1989; Furtula et al., 1990) have all shown results which suggest that lipid microdomains are present at the nanometric dimension. These results, however, are indirect and therefore are open to interpretation. Because of their small size, lipid microdomains will be difficult to access within the spatial resolution constraints governing conventional optical microscopy, and AFM measurements will be complicated by the complex surface topography encountered in natural membranes. The results shown here, however, suggest that NSOM may provide the capabilities needed to bridge this gap and probe the small microdomains present in biomembranes at the nanometer level.

CONCLUSIONS

The lipid phase structure in LB monolayers and bilayers of DPPC fluorescently doped with 0.25 mol% diI_{C18} are studied with the high spatial resolution of confocal microscopy, AFM, and NSOM. At a spatial resolution beyond that possible with confocal microscopy, small lipid domains are seen with both AFM and NSOM in monolayers formed at a surface pressure of 9 mN/m. Comparison of the height and fluorescence images collected with NSOM is used to confirm that the small domains are distinct lipid phases and not simply defects in the monolayer. For bilayers, both confocal microscopy and AFM are unable to visualize the small domains present in the film—confocal because of limitations in spatial resolution, and AFM because of the complex surface topography of the bilayers. NSOM, on the other hand, provides a high-resolution fluorescence mapping of the underlying phase structure in the bilayer that is not immediately apparent in the topography image. It is also shown that both sides of the bilayer can be selectively probed by controlling which side contains the fluorescent probe molecule. The insensitivity of the phase structure to transfer methods suggests that the small coexisting LC and LE domains are not a result of the film transfer process, but instead arise from a thinning of the water layer after transfer to the solid support. Results from these and other studies suggest that the small domains are not present at the air-water interface, but are introduced into the film after transfer to the substrate. NSOM studies are currently being conducted on lipid films at the air/water interface in the effort to resolve this issue. Taken together, these results suggest that NSOM may be uniquely sensitive to the phase structure present in lipid bilayers at the nanometer scale and may provide new clues to the existence of lipid phase domains in natural biomembranes.

We thank Chad Talley for the helpful comments and modifications to the LB trough that allow for Langmuir-Schaefer film transfer, and Digital Instruments for the technical advice.

We gratefully acknowledge the support of the National Science Foundation (CHE-9612730) and the Searle Scholars Program/The Chicago Community Trust.

REFERENCES

- Ambrose, W. P., P. M. Goodwin, J. C. Martin, and R. A. Keller. 1994. Alterations of single molecule fluorescence lifetimes in near-field optical microscopy. *Science*. 265:364–367.
- Baeza, I., C. Wong, R. Mondragon, S. Gonzalez, M. Ibanez, N. Farfan, and C. Arguello. 1994. Transbilayer diffusion of divalent cations into liposomes mediated by lipidic particles of phosphatidate. *J. Mol. Evol.* 39:560–568.
- Baldwin, P. A., and W. Hubbell. 1985. Effects of lipid environment on the light-induced conformational changes of rhodopsin. 2. Roles of lipid chain length, unsaturation, and phase state. *Biochemistry*. 24:2633–2639.
- Betzig, E., and R. J. Chichester. 1993. Single molecules observed by near-field scanning optical microscopy. *Science*. 262:1422–1425.
- Betzig, E., R. J. Chichester, F. Lanni, and D. L. Taylor. 1993. Near-field fluorescence imaging of cytoskeletal actin. *Bioimaging*. 1:129–135.
- Betzig, E., J. K. Trautman, T. D. Harris, J. S. Weiner, and R. L. Kostelak. 1991. Breaking the diffraction barrier: optical microscopy on a nanometric scale. *Science*. 251:1468–1470.
- Bhushan, B., J. N. Israelachvili, and U. Landman. 1995. Nanotribology: friction, wear and lubrication at the atomic scale. *Nature*. 374:607–616.
- Bourdieu, L., O. Ronsin, and D. Chatenay. 1993. Molecular positional order in Langmuir-Blodgett films by atomic force microscopy. *Science*. 259:798–801.
- Buratto, S. K., J. W. P. Hsu, J. K. Trautman, E. Betzig, R. B. Bylisma, C. C. Bahr, and M. J. Cardillo. 1994. Imaging InGaAsP quantum-well lasers using near-field scanning optical microscopy. *J. Appl. Phys.* 76:7720–7725.
- Cadenhead, D. A., F. Müller-Landau, and B. M. J. Kellner. 1980. Phase transitions in insoluble one- and two-component films at the air/water interface. In *Ordering in Two Dimensions*. S. K. Sinha, editor. Elsevier, Amsterdam. 73.
- Caffrey, M., and G. W. Feigenson. 1981. Fluorescence quenching in model membranes. 3. Relationship between calcium adenosinetriphosphatase enzyme activity and the affinity of the protein for phosphatidylcholines with different acyl chain characteristics. *Biochemistry*. 20:1949–1961.
- Chen, Y. L. E., M. L. Gee, C. A. Helm, J. N. Israelachvili, and P. M. McGuiggan. 1989. Effects of humidity on the structure and adhesion of amphiphilic monolayers on mica. *J. Phys. Chem.* 93:7057–7059.
- Chernomordik, L. V., and J. Zimmerberg. 1995. Bending membranes to the task: structural intermediates in bilayer fusion. *Curr. Opin. Struct. Biol.* 5:541–547.
- Chi, L. F., M. Anders, H. Fuchs, R. R. Johnston, and H. Ringsdorf. 1993. Domain structures in Langmuir-Blodgett films investigated by atomic force microscopy. *Science*. 259:213–216.
- Criado, M., H. Eibl, and F. J. Barrantes. 1984. Functional properties of the acetylcholine receptor incorporated in model lipid membranes. *J. Biol. Chem.* 259:9188–9198.
- Derzko, Z., and K. Jacobson. 1980. Comparative lateral diffusion of fluorescent lipid analogues in phospholipid multibilayers. *Biochemistry*. 19:6050–6057.
- Dufrene, Y. F., W. R. Barger, J. B. D. Green, and G. U. Lee. 1997. Nanometer-scale surface properties of mixed phospholipid monolayers and bilayers. *Langmuir*. 13:4779–4784.
- Dugas, C. M., Q. Li, I. A. Khan, and E. A. Nothnagel. 1989. Lateral diffusion in the plasma membrane of maize protoplasts with implications for cell culture. *Planta*. 179:387–396.
- Dunn, R. C., E. V. Allen, S. A. Joyce, G. A. Anderson, and X. S. Xie. 1995. Near-field fluorescent imaging of single proteins. *Ultramicroscopy*. 57:113–117.
- Dunn, R. C., G. H. Holtom, L. Mets, and X. S. Xie. 1994. Near-field fluorescence imaging and fluorescence lifetime measurements of light harvesting complexes in intact photosynthetic membranes. *J. Phys. Chem.* 98:3094–3098.
- Dupou, L., A. Lopez, and J.-L. Tocanne. 1988. Comparative study of the lateral motion of extrinsic probes and anthracene-labelled constitutive phospholipids in the plasma membrane of Chinese hamster ovary cells. *Eur. J. Biochem.* 171:669–674.
- Enderle, T., T. Ha, D. F. Ogletree, D. S. Chemla, C. Magowan, and S. Weiss. 1997. Membrane specific mapping and colocalization of malarial and host skeletal proteins in the *Plasmodium falciparum* infected erythrocyte by dual-color near-field scanning optical microscopy. *Proc. Natl. Acad. Sci. USA*. 94:520–525.
- Epand, R. M., and R. F. Epand. 1994. Calorimetric detection of curvature strain in phospholipid bilayers. *Biophys. J.* 66:1450–1456.
- Fang, J., and C. M. Knobler. 1995. Control of density in self-assembled organosilane monolayers by Langmuir-Blodgett deposition. *J. Phys. Chem.* 99:10425–10429.
- Fang, Y., and J. Yang. 1997. The growth of bilayer defects and the induction of interdigitated domains in the lipid-loss process of supported phospholipid bilayers. *Biochim. Biophys. Acta*. 1324:309–319.
- Furtula, V., I. A. Khan, and E. A. Nothnagel. 1990. Selective osmotic effect on diffusion of plasma membrane lipids in maize protoplasts. *Proc. Natl. Acad. Sci. USA*. 87:6532–6536.
- Gaines, G. L. 1966. *Insoluble Monolayers at Gas Liquid Interfaces*. Interscience, New York.

- Gennis, R. B. 1989. *Biomembranes: Molecular Structure and Function*. Springer Verlag, New York.
- Gibson, N. J., and M. F. Brown. 1993. Lipid headgroup and acyl chain composition modulate the M1-MII equilibrium of rhodopsin in recombinant membranes. *Biochemistry*. 32:2438–2454.
- Grober, R. D., T. D. Harris, J. K. Trautman, E. Betzig, W. Wegscheider, L. Pfeiffer, and K. West. 1994. Optical spectroscopy of a GaAs/AlGaAs quantum wire structure using near-field scanning optical microscopy. *Appl. Phys. Lett.* 64:1421–1423.
- Ha, T., T. Enderle, D. F. Ogletree, D. S. Chemla, P. R. Selvin, and S. Weiss. 1996. Probing the interaction between two single molecules: fluorescence resonance energy transfer between a single donor and a single acceptor. *Proc. Natl. Acad. Sci. USA*. 93:6264–6268.
- Harris, T. D., D. Gershoni, R. D. Grober, L. Pfeiffer, W. K., and N. Chand. 1996. Near-field optical spectroscopy of single quantum wires. *Appl. Phys. Lett.* 68:988–990.
- Higgins, D. A., and P. F. Barbara. 1995. Excitonic transitions in J-aggregates probed by near-field scanning optical microscopy. *J. Phys. Chem.* 99:3–7.
- Hollars, C. W., and R. C. Dunn. 1997. Submicron fluorescence, topology and compliance measurements of phase separated lipid monolayers using tapping-mode near-field scanning optical microscopy. *J. Phys. Chem.* 101:6313–6317.
- Hui, S., and A. Sen. 1989. Effects of lipid packing on polymorphic phase behavior and membrane properties. *Proc. Natl. Acad. Sci. USA*. 86:5825–5829.
- Hwang, J., L. K. Tamm, C. Bohm, T. Ramalingam, E. Betzig, and M. Edidin. 1995. Nanoscale complexity of phospholipid monolayers investigated by near-field scanning optical microscopy. *Science*. 270:610–614.
- Jensen, J. W., and J. S. Schutzbach. 1984. Activation of mannosyltransferase II by nonbilayer phospholipids. *Biochemistry*. 23:1115–1119.
- Johannsson, A., G. A. Smith, and J. C. Metcalfe. 1981. The effect of bilayer thickness on the activity of $(\text{Na}^{++}\text{K}^{+})$ -ATPase. *Biochim. Biophys. Acta*. 641:416–421.
- Johnson, M., and M. Edidin. 1978. Lateral diffusion in plasma membrane of mouse egg is restricted after fertilisation. *Nature*. 272:448–450.
- Kelusky, E. C., and I. C. P. Smith. 1983. Characterization of the binding of the local anesthetics procaine and tetracaine to model membranes of phosphatidylethanolamine: a deuterium nuclear magnetic resonance study. *Biochemistry*. 22:6011–6017.
- Knapp, H. F., W. Wiegrabe, M. Heim, R. Eschrich, and R. Guckenberger. 1995. Atomic force microscope measurements and manipulation of Langmuir-Blodgett films with modified tips. *Biophys. J.* 69:708–715.
- Knobler, C. M. 1990. Seeing phenomena in the flatland: studies of monolayers by fluorescence microscopy. *Science*. 249:870–874.
- Lehtonen, J. Y. A., and P. K. J. Kinnunen. 1995. Poly(ethyleneglycol)-induced and temperature-dependent phase separation in fluid binary phospholipid membranes. *Biophys. J.* 68:525–535.
- Lösche, M., J. Rabe, A. Fischer, B. U. Rucha, W. Knoll, and H. Möhwald. 1984. Microscopically observed preparation of Langmuir-Blodgett films. *Thin Solid Films*. 117:269–280.
- Lösche, M., E. Sackmann, and H. Möhwald. 1983. A fluorescence microscopic study concerning the phase diagram of phospholipids. *Ber. Bunsenges. Phys. Chem.* 87:848–852.
- Lundbaek, J. A., P. Birn, J. Girshman, A. J. Hansen, and O. S. Anderson. 1996. Membrane stiffness and channel function. *Biochemistry*. 35:3825–3830.
- Masai, J., T. Shibata-Seki, K. Sasaki, H. Murayama, and K. Sano. 1996. Scanning force microscopy characterization of thin lipid films on a substrate. *Thin Solid Films*. 273:289–296.
- McCallum, C. D., and R. M. Epand. 1995. Insulin receptor autophosphorylation and signaling is altered by modulation of membrane physical properties. *Biochemistry*. 34:1815–1824.
- McConnell, H. M. 1991. Structures and transitions in lipid monolayers at the air-water interface. *Annu. Rev. Phys. Chem.* 42:171–195.
- McConnell, H. M., L. K. Tamm, and R. M. Weis. 1984. Periodic structures in lipid monolayer phase transitions. *Proc. Natl. Acad. Sci. USA*. 81:3249–3253.
- Metcalfe, T. N., III, J. L. Wang, and M. Schindler. 1986. Lateral diffusion of phospholipids in the plasma membrane of soybean protoplasts: evidence for membrane lipid domains. *Proc. Natl. Acad. Sci. USA*. 83:95–99.
- Mikrut, J. M., P. Dutta, J. B. Ketterson, and R. C. MacDonald. 1993. Atomic-force and fluorescence microscopy of Langmuir-Blodgett monolayers of L-dimyristoylphosphatidic acid. *Phys. Rev. B*. 48:14479–14487.
- Moers, M. H. P., H. E. Gaub, and N. F. van Hulst. 1994. Poly(diacetylene) monolayers studied with a fluorescence near-field optical microscope. *Langmuir*. 10:2774–2777.
- Möhwald, H. 1990. Phospholipid and phospholipid-protein monolayers at the air/water interface. *Annu. Rev. Phys. Chem.* 41:441–476.
- Muramatsu, H., N. Chiba, K. Homma, K. Nakajima, T. Ataka, S. Ohta, A. Kusumi, and M. Fujihira. 1995. Near-field optical microscopy in liquids. *Appl. Phys. Lett.* 66:3245–3247.
- Navarro, J., M. Toivio-Kinnucan, and E. Racker. 1984. Effect of lipid composition on the calcium/adenosine 5'-triphosphate coupling ratio of the Ca^{2+} -ATPase of sarcoplasmic reticulum. *Biochemistry*. 23:130–135.
- Overney, R. M., E. Meyer, J. Frommer, D. Brodbeck, R. Luthi, L. Howald, H. J. Guntherodt, M. Fujihira, H. Takano, and Y. Gotoh. 1992. Friction measurements on phase-separated thin films with a modified atomic force microscope. *Nature*. 359:133–135.
- Paesler, M. A., and P. J. Moyer. 1996. *Near-Field Optics: Theory, Instrumentation, and Applications*. John Wiley and Sons, New York.
- Peschke, J., J. Riegler, and H. Möhwald. 1987. Quantitative analysis of membrane distortions induced by mismatch of protein and lipid hydrophobic thickness. *Eur. Biophys. J.* 14:385–391.
- Peterson, N. O., and W. B. McConnaughy. 1981. Effects of multiple membranes on measurements of cell surface dynamics by fluorescence photobleaching. *J. Supramol. Struct. Cell. Biochem.* 17:213–221.
- Pohl, D. W. 1991. Scanning near-field optical microscopy (SNOM). In *Advances in Optical, and Electron Microscopy*, Vol. 12. T. Mulvey and C. J. R. Sheppard, editors. Academic Press, London. 243–312.
- Reiter, G. 1992. Dewetting of thin polymer films. *Phys. Rev. Lett.* 68:75–78.
- Riegler, H., and K. Spratte. 1992. Structural changes in lipid monolayers during the Langmuir-Blodgett transfer due to substrate/monolayer interactions. *Thin Solid Films*. 210–211:9–12.
- Riegler, J. E., and J. D. LeGrange. 1988. Observation of a monolayer phase transition on the meniscus in a Langmuir-Blodgett transfer configuration. *Phys. Rev. Lett.* 61:2492–2495.
- Rilfors, L., J. B. Hauksson, and G. Lindblom. 1994. Regulation and phase equilibria of membrane lipids from *Bacillus megaterium* and *Acholeplasma laidlawii* strain A containing methyl-branched acyl chains. *Biochemistry*. 33:6110–6120.
- Roberts, G. 1990. *Langmuir-Blodgett Films*. Plenum Press, New York.
- Sackmann, E. 1994. Membrane bending energy concept of vesicle and cell shapes and shape transitions. *FEBS Lett.* 346:3–16.
- Sackmann, E. 1996. Supported membranes: scientific and practical applications. *Science*. 271:43–48.
- Salamon, Z., Y. Wang, M. F. Brown, H. A. Macleod, and G. Tollin. 1994. Conformational changes in rhodopsin probed by surface plasmon resonance spectroscopy. *Biochemistry*. 33:13706–13711.
- Santesson, L., T. M. H. Wong, M. Taborelli, and P. Descouts. 1995. Scanning force microscopy characterization of Langmuir-Blodgett films of sulfur-bearing lipids on mica and gold. *J. Phys. Chem.* 99:1038–1045.
- Shiku, H., and R. C. Dunn. 1998. Direct observation of DPPC phase domain motion on mica surfaces under conditions of high relative humidity. *J. Phys. Chem. B*. 102:3791–3797.
- Sikes, H. D., and D. K. Schwartz. 1997. A temperature-dependent two-dimensional condensation transition during Langmuir-Blodgett deposition. *Langmuir*. 13:4704–4709.
- Sikes, H. D., J. T. Woodward, and D. K. Schwartz. 1996. Pattern formation in a substrate-induced phase transition during Langmuir-Blodgett transfer. *J. Phys. Chem.* 100:9093–9097.
- Spratte, K., and H. Riegler. 1994. Steady state morphology and composition of mixed monomolecular films (Langmuir monolayers) at the air/water interface in the vicinity of the three-phase line: model calculations and experiments. *Langmuir*. 10:3161–3173.

- Srinivasan, M. P., B. G. Higgins, and P. Stroeve. 1988. Entrainment of aqueous subphase in Langmuir-Blodgett films. *Thin Solid Films*. 159: 191–205.
- Swalen, J. D., D. L. Allara, J. D. Andrade, E. A. Chandross, S. Garoff, J. Israelachvili, T. J. McCarthy, R. Murray, R. F. Pease, J. F. Rabolt, K. J. Wynne, and H. Yu. 1987. Molecular monolayers and films. *Langmuir*. 3:932–950.
- Talley, C. E., G. Cooksey, and R. C. Dunn. 1996. High resolution fluorescence imaging with cantilevered near-field fiber optic probes. *Appl. Phys. Lett.* 69:3809–3811.
- Tamm, L. K., C. Bohm, J. Yang, Z. Shao, J. Hwang, M. Ediden, and B. Betzig. 1996. Nanostructure of supported phospholipid monolayers and bilayers by scanning probe microscopy. *Thin Solid Films*. 284–285: 813–816.
- Tocanne, J.-F., L. Dupou-Cezanne, and A. Lopez. 1994. Lateral diffusion of lipids in model and natural membranes. *Prog. Lipid Res.* 33:203–237.
- Tollner, K., R. Popovitz-Biro, M. Lahav, and D. Milstein. 1997. Impact of molecular order in Langmuir-Blodgett films on catalysis. *Science*. 278: 2100–2102.
- Trautman, J. K., J. J. Macklin, L. E. Brus, and E. Betzig. 1994. Near-field spectroscopy of single molecules at room temperature. *Nature*. 369: 40–42.
- van Hulst, N. F., and M. H. P. Moers. 1996. Biological applications of near-field optical microscopy. *IEEE Eng. Med. Biol.* 15:51–57.
- Vaz, W. L. C., and P. F. F. Almeida. 1993. Phase topology and percolation in multi-phase lipid bilayers: is the biological membrane a domain mosaic? *Curr. Opin. Struct. Biol.* 3:482–488.
- Walko, R. M., and E. A. Nothnagel. 1989. Lateral diffusion of proteins and lipids in the plasma membrane of rose protoplast. *Protoplasma*. 152: 46–56.
- Wolf, D. E., A. C. Lipscomb, and V. M. Maynard. 1988. Causes of nondiffusing lipid in the plasma membrane of mammalian spermatozoa. *Biochemistry*. 27:860–865.
- Xie, X. S., and R. C. Dunn. 1994. Probing single molecule dynamics. *Science*. 265:361–364.
- Yang, X. M., D. Xiao, Z. H. Lu, and Y. Wei. 1995. Structural investigation of Langmuir-Blodgett monolayers of L- α -dipalmitoylphosphatidylcholine by atomic force microscopy. *Appl. Surf. Sci.* 90:175–183.
- Yang, X. M., D. Xiao, S. J. Xiao, Z. H. Lu, and Y. Wei. 1994a. Observation of chiral domain morphology in a phospholipid Langmuir-Blodgett monolayer by atomic force microscopy. *Phys. Lett. A*. 193:195–198.
- Yang, X. M., D. Xiao, S. J. Xiao, and Y. Wei. 1994b. Domain structures of phospholipid monolayer Langmuir-Blodgett films determined by atomic force microscopy. *Appl. Phys. A*. 59:139–143.